

# Study on asymptotic analytical solutions using HAM for strongly nonlinear vibrations of a restrained cantilever beam with an intermediate lumped mass

Y. H. Qian · S. K. Lai · W. Zhang · Y. Xiang

Received: 7 October 2010 / Accepted: 28 February 2011 /  
Published online: 31 March 2011  
© Springer Science+Business Media, LLC 2011

**Abstract** Presented herein is to establish the asymptotic analytical solutions for the fifth-order Duffing type temporal problem having strongly inertial and static nonlinearities. Such a problem corresponds to the strongly nonlinear vibrations of an elastically restrained beam with a lumped mass. Taking into consideration of the inextensibility condition and using an assumed single mode Lagrangian method, the single-degree-of-freedom ordinary differential equation can be derived from the governing equations of the beam model. Various parameters of the nonlinear unimodal temporal equation stand for

---

Y. H. Qian · W. Zhang (✉)  
College of Mechanical Engineering, Beijing University of Technology,  
Beijing 100124, People's Republic of China  
e-mail: sandyzhang0@yahoo.com

Y. H. Qian  
e-mail: zjjhgyh@yahoo.com

Y. H. Qian  
College of Mathematics, Physics and Information Engineering,  
Zhejiang Normal University, Jinhua, Zhejiang 321004, People's Republic of China

Y. Xiang  
School of Engineering, University of Western Sydney, Locked Bag 1797,  
Penrith South DC, Sydney, NSW 1797, Australia

S. K. Lai · Y. Xiang  
Centre for Civionics Research, University of Western Sydney, Locked Bag 1797,  
Penrith South DC, Sydney, NSW 1797, Australia

*Present Address:*

S. K. Lai  
Department of Mechanical Engineering, The University of Hong Kong,  
Pokfulam Road, Hong Kong, People's Republic of China

different vibration modes of inextensible cantilever beam. By imposing the homotopy analysis method (HAM), we establish the asymptotic analytical approximations for solving the fifth-order nonlinear unimodal temporal problem. Within this research framework, both the frequencies and periodic solutions of the nonlinear unimodal temporal equation can be explicitly and analytically formulated. For verification, numerical comparisons are conducted between the results obtained by the homotopy analysis and numerical integration methods. Illustrative examples are selected to demonstrate the accuracy and correctness of this approach. Besides, the optimal HAM approach is introduced to accelerate the convergence of solutions.

**Keywords** Strongly nonlinear vibration · Homotopy analysis method · Restrained cantilever beam · Lumped mass · Fifth-order temporal equation

**Mathematics Subject Classifications (2010)** 34A34 · 34C25 · 70K05

## 1 Introduction

Nonlinear dynamical problems pervade in numerous disciplines of science and engineering, such as in mechanical, physical and structural applications, and even in aeronautical technology. Theoretically, most of the nonlinear dynamical models are governed by a set of differential equations and auxiliary conditions that arise from modeling processes [22]. By investigating the steady-state and transient responses of nonlinear differential equations, the quest of accurate analytical or semi-analytical techniques is highly indispensable. In contrast with the numerical analysis, the scientific merit of the analytical solutions provides a superior understanding and insight of the interrelationship between the governing parameters and resulting solutions, such that the availability of the design practices in science and engineering can be advanced and benefited.

Over the past few decades, many ingenious analytical methods have been developed for solving different kinds of strongly nonlinear equations, such as the modified perturbation methods [2, 5, 25, 27] and improved harmonic balance methods [11, 26, 28, 32]. Meanwhile, the homotopy analysis method (HAM) [15–17] was emerged as one of the robust and efficient analytical techniques in solving nonlinear problems. The rationale behind the HAM stems from the homotopy [9] that is a significant concept in topology [23]. It has been generalized to tackle various nonlinear problems in solid and fluid mechanics [1, 4, 12, 31, 33, 34]. Moreover, it goes beyond the conventional perturbation methods, which are only restricted to address the problems with weak nonlinearities [17]. Thus, this paper attempts to use the HAM for dealing with the fifth-order Duffing type temporal problem containing strongly inertial and static nonlinearities [8].

The underlying implication of this fifth-order nonlinear problem corresponds to the nonlinear vibration of a restrained cantilever beam with an intermediate lumped mass [8]. The investigation of cantilever beam models is mainly due to its significance and relevance in contemporary engineering structures, such as a cantilever bridge. Formerly, there have been extensive research subjects in regard to the dynamic behaviour of assorted cantilever beam problems. For instance, Hamdan and Dado [7] investigated the flexural large amplitude vibration of a cantilever beam attaching a lumped mass with a rotary inertia, Zhang et al. [35] analyzed the global bifurcation and chaotic dynamics for the nonlinear nonplanar oscillation of a cantilever beam stimulated by harmonic axial and transverse excitations at the free end, Hu et al. [10] studied the principal resonance of an Euler–Bernoulli cantilever with a contact end, and recently Ke et al. [13] revealed the vibration and buckling behaviour of a functionally graded cantilever beam with open edge cracks.

In considering the inextensibility condition of the elastically restrained cantilever beam, Hamdan and Shabahen [8] not only formulated the fifth-order nonlinear problem by means of the Euler–Lagrange equation, but also employed the time transformation approach to obtain the approximate solutions for the period of oscillation. Without taking into account the inextensibility condition, the inertial nonlinear terms do not exist in the fifth-order Duffing type temporal problem. This nonlinear equation can be simply designated as the cubic–quintic Duffing oscillator, which has been treated by the time transformation approach [8], Newton harmonic balance method [14, 20], and homotopy padé technique [24].

The fifth-order Duffing type problem governed by the inertial and static nonlinear terms is much more complicated in general. Recently, a number of scholars have attempted to solve this nonlinear problem. For instance, Chen and Chen [3] applied the differential transformation method to cope with this fifth-order nonlinear problem. Subsequently, Mehdipour et al. [21] and Ganji et al. [6], respectively, adopted the energy balance method, amplitude–frequency formulation and homotopy perturbation method to yield the lower-order approximate solutions for this strongly nonlinear problem. However, the lower-order approximate solutions may not always achieve the desired accuracy for large amplitudes of oscillation as well as large governing parameters.

The prime objective of this paper is to explore the utility of the HAM for the fifth-order strongly nonlinear problem. The paper is organized as follows. The derivation of the strongly nonlinear equation from the governing equations of the beam model is described in Section 2 in brief. In Section 3, the HAM is utilized to establish the asymptotic analytical solutions via the construction of the higher-order analytical approximations. In addition, the optimal HAM approach used to accelerate the convergence of solutions is also provided and discussed. The numerical results of the HAM are presented and compared with respect to the numerical integration solutions in Section 4. Finally, a conclusion summarizes the research findings in Section 5.

### 2 Mathematical formulation

In favour of integrity and completeness throughout the context, the mathematical formulation of the fifth-order Duffing type temporal problem having strongly inertial and static nonlinearities [8] is briefly mentioned herein as a reference. Consider an isotropic slender beam with uniform length  $l$  and mass  $m$  per unit length as shown in Fig. 1 [8]. It is supposed that the beam thickness is very small as compared to the beam length, thus the effects of rotary inertia and shear deformation can be neglected. The dimensionless beam tip displacement is  $a = b/l$  and the angle of inclination is  $\theta$ . For the boundary constraints, one of the supporting ends is hinged at the base to a rotational spring with stiffness  $K$ , and the other end is free. Besides, the intermediate lumped mass  $M$  is also attached at  $s = d$  along the beam span.

The kinetic energy ( $T$ ) and strain energy ( $V$ ) of the flexural vibration of the beam in Fig. 1 are expressed as [8, 30]

$$T = \frac{ml}{2} \int_0^1 [1 + \mu \delta(\xi - \eta)] (\dot{x}^2 + \dot{y}^2) d\xi \tag{1}$$

and

$$V = \frac{EI}{2} \int_0^1 R^2(\xi, t) d\xi \tag{2}$$

where  $\mu = M/(ml)$  is the dimensionless mass ratio parameter,  $\delta(\xi - \eta)$  is Dirac's function with  $\xi = s/l$  and  $\eta = d/l$  being the dimensionless arc length and the dimensionless relative position of the lumped mass  $M$  respectively,  $EI$  is the modulus of flexural rigidity, and  $R = \lambda^3 (x'y'' - x''y')$  [30] is the curvature of the central line of the beam with  $\lambda = 1/l$ . A dot denotes the derivative

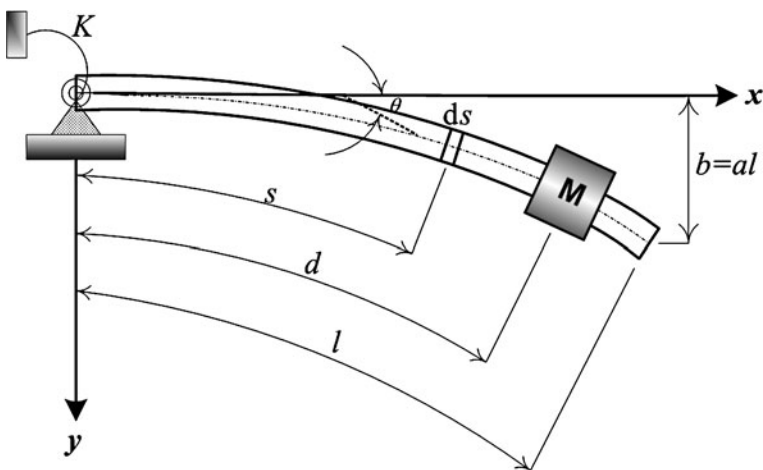


Fig. 1 Geometry and coordinate system for a beam with a lumped mass

with respect to time  $t$ , and a prime denotes the derivative with respect to the dimensionless arc length  $\xi$ .

In Eq. 2, the curvature  $R = \lambda^3 (x' y'' - x'' y')$  can be further written in terms of  $y'$  and  $y''$  only by using the subsidiary condition, which is  $x'^2 + y'^2 = l^2$  [30] to eliminate  $x'$  and  $x''$  as [7]

$$V = \frac{EI\lambda^3}{2} \int_0^1 \left( \frac{1}{1 - \lambda^2 y'^2} \right) [(1 - \lambda^2 y'^2) y'' + \lambda^2 y'^2 y''']^2 d\xi \tag{3}$$

Assuming  $(\lambda y')^2 \ll 1$ , the term  $1/(1 - \lambda^2 y'^2)$  in Eq. 3 can be expanded into a power series up to fifth order [8]

$$V = \frac{EI\lambda^3}{2} \int_0^1 (y'^2 + \lambda^2 y'^2 y''^2 + \lambda^4 y'^4 y''^2) d\xi \tag{4}$$

In accordance with the inextensibility condition of the beam, it means that the length of the neutral axis keeps constant and the following relation is constrained [7, 8]

$$(1 + \lambda x')^2 + (\lambda y')^2 = 1 \text{ or } 1 + \lambda x' = \sqrt{1 - (\lambda y')^2} \tag{5}$$

Supposing again  $(\lambda y')^2 \ll 1$  and expanding  $\sqrt{1 - (\lambda y')^2}$  into a power series up to fifth order, we can integrate  $x'$  to have [8]

$$x = -\frac{1}{2} \int_0^\xi \left( \lambda y'^2 + \frac{1}{4} \lambda^3 y'^4 \right) dx \tag{6}$$

In Eq. 1, the term  $\dot{x}$  can be computed by differentiating Eq. 6 with respect to time  $t$ .

The Lagrangian of the beam (i.e.  $L = T - V$ ) can be formulated by substituting the approximate unimodal solution for  $y(\xi, t) = \phi(\xi) u(t)$ , in which  $\phi(\xi)$  is the normalized eigenfunction of the associated linear problem and  $u(t)$  is the time function to be sought. Having conducted some manipulations, one obtains [8]

$$L = \frac{ml}{2} \left[ \alpha_1 \dot{u}^2 + \alpha_3 \lambda^2 u^2 \dot{u}^2 + \alpha_4 \lambda^2 u^2 \dot{u}^2 + \alpha_5 \lambda^4 u^4 \dot{u}^2 + \alpha_6 \lambda^4 u^4 \dot{u}^2 - \frac{EI\lambda^4}{m} (\alpha_2 u^2 + \alpha_7 \lambda^2 u^4 + \alpha_8 \lambda^4 u^6) \right] \tag{7}$$

in which  $\lambda$  is assumed to be unity.

Based on the Euler–Lagrange differential equation, the fifth-order Duffing type temporal problem having strongly inertial and static nonlinearities can be derived from Eq. 7 as follows [8]

$$\ddot{\bar{x}} + \bar{x} + \varepsilon_1 \bar{x}^2 \ddot{\bar{x}} + \varepsilon_1 \bar{x} \dot{\bar{x}}^2 + \varepsilon_2 \bar{x}^4 \ddot{\bar{x}} + 2\varepsilon_2 \bar{x}^3 \dot{\bar{x}}^2 + \varepsilon_3 \bar{x}^3 + \varepsilon_4 \bar{x}^5 = 0 \tag{8}$$

where  $\bar{x}$  is the dimensionless deflection at the beam tip, and  $\varepsilon_1, \varepsilon_2, \varepsilon_3$  and  $\varepsilon_4$  are functions of  $\alpha_i$  ( $i = 1-8$ ) in Eq. 7.

Whereas the parameters  $\alpha_i$  ( $i = 1-8$ ) are functions of the mode shape functions  $\phi$ , thus, special values of  $\varepsilon_1, \varepsilon_2, \varepsilon_3$  and  $\varepsilon_4$  stand for different vibration modes. The detailed explanation of  $\alpha_i$  ( $i = 1-8$ ) and  $\phi$  was discussed in Ref. [8]. Undergoing the inextensibility condition, the first four strongly nonlinear terms of inertia type (i.e.  $\varepsilon_1 \bar{x}^2 \ddot{\bar{x}}, \varepsilon_1 \bar{x} \dot{\bar{x}}^2, \varepsilon_2 \bar{x}^4 \ddot{\bar{x}}$  and  $2\varepsilon_2 \bar{x}^3 \dot{\bar{x}}^2$ ) are presented in Eq. 8. These terms are also due to the kinetic energy of axial motion. While the last two nonlinear terms  $\varepsilon_3 \bar{x}^3$  and  $\varepsilon_4 \bar{x}^5$  are strongly static nonlinearities caused by the potential energy stored in bending. In Eq. 8, the initial conditions are assumed to be subjected as follows [6]

$$\bar{x}(0) = A, \dot{\bar{x}}(0) = 0 \tag{9}$$

It is noted that a dot in Eqs. 8 and 9 denotes the derivative with respect to the dimensionless time  $\bar{t}$ . For simplicity and convenience, the overhead bars of  $\bar{x}$  and  $\bar{t}$  are ignored and written as  $x$  and  $t$  in the subsequent solution methodology and results.

### 3 Solution methodology

In what follows, the HAM [15–17] is applied to solve Eq. 8 analytically. By introducing a new variable  $\tau = \omega t$  and substituting it into Eq. 9, one obtains

$$\omega^2 x'' + x + \varepsilon_1 \omega^2 x^2 x'' + \varepsilon_1 \omega^2 x x'^2 + \varepsilon_2 \omega^2 x^4 x'' + 2\varepsilon_2 \omega^2 x^3 x'^2 + \varepsilon_3 x^3 + \varepsilon_4 x^5 = 0 \tag{10}$$

$$x(0) = A, x'(0) = 0 \tag{11}$$

where a prime denotes the derivative with respect to  $\tau$ , and  $\omega$  is the nonlinear frequency.

It is known that the oscillation of a conservative system without damping effect is a periodic motion of  $\tau$  of period  $2\pi$ . The harmonic function is the simplest type for this periodic motion. Hence, the displacement solution in Eq. 10 can be expressed by the following base functions

$$\{\cos(2m - 1)\tau | m = 1, 2, 3, \dots\} \tag{12}$$

In order to satisfy the initial conditions in Eq. 11, the initial guess of  $x(\tau)$  for the zeroth-order deformation equation is chosen as follows

$$x_0(\tau) = A \cos \tau \tag{13}$$

To construct the homotopy function, the auxiliary linear operator of a conservative system is selected as

$$L[x(\tau; q)] = \omega_0^2 \left( \frac{\partial^2 x(\tau; q)}{\partial \tau^2} + x(\tau; q) \right) \tag{14}$$

The auxiliary linear operator  $L$  is chosen in such a way that all solutions of the corresponding high-order formation equations are existed and can be

expressed by the general form of the base function. In Eq. 10, the nonlinear operator is written as

$$\begin{aligned}
 N[x(\tau; q), \omega(q)] = & \omega^2 \frac{\partial^2 x(\tau; q)}{\partial \tau^2} + x(\tau; q) + \varepsilon_1 \omega^2 [x(\tau; q)]^2 \frac{\partial^2 x(\tau; q)}{\partial \tau^2} \\
 & + \varepsilon_1 \omega^2 x(\tau; q) \left[ \frac{\partial x(\tau; q)}{\partial \tau} \right]^2 + \varepsilon_2 \omega^2 [x(\tau; q)]^4 \frac{\partial^2 x(\tau; q)}{\partial \tau^2} \\
 & + 2\varepsilon_2 \omega^2 [x(\tau; q)]^3 \left[ \frac{\partial x(\tau; q)}{\partial \tau} \right]^2 + \varepsilon_3 [x(\tau; q)]^3 + \varepsilon_4 [x(\tau; q)]^5
 \end{aligned}
 \tag{15}$$

In accordance with the HAM, the zeroth-order deformation equation is constructed into the following form,

$$(1 - q) L[x(\tau; q) - x_0(\tau)] = q\hbar N[x(\tau; q)]
 \tag{16}$$

where  $q \in [0,1]$  and  $\hbar$  are, respectively, embedding and convergence-control parameters.

As  $q$  changes from 0 to 1,  $x(\tau; q)$  varies from the initial guess  $x_0(\tau)$  to the unknown solution  $x(\tau)$ . Similarly,  $\omega(q)$  varies from the initial guess frequency  $\omega_0$  to the physical frequency  $\omega$ .

Using the Taylor series expansion yields

$$x(\tau; q) = x_0(\tau) + \sum_{m=1}^{+\infty} x_m(\tau) q^m
 \tag{17}$$

$$\omega(q) = \omega_0 + \sum_{m=1}^{+\infty} \omega_m q^m
 \tag{18}$$

in which

$$x_m(\tau) = \frac{1}{m!} \left. \frac{\partial^m x(\tau; q)}{\partial q^m} \right|_{q=0}
 \tag{19}$$

$$\omega_m = \frac{1}{m!} \left. \frac{\partial^m \omega(q)}{\partial q^m} \right|_{q=0}
 \tag{20}$$

Suppose that  $\hbar$  is properly chosen, the power series solutions in Eqs. 17 and 18 can be converged at  $q = 1$ , Eqs. 17 and 18 then become

$$x(\tau) = x_0(\tau) + \sum_{m=1}^{+\infty} x_m(\tau)
 \tag{21}$$

$$\omega = \omega_0 + \sum_{m=1}^{+\infty} \omega_m
 \tag{22}$$

For the sake of simplicity, we define the following vectors

$$\mathbf{u}_n = \{x_1(\tau), x_2(\tau), \dots, x_n(\tau)\}, \quad \boldsymbol{\omega}_n = \{\omega_0, \omega_1, \dots, \omega_n\} \tag{23}$$

By differentiating the zeroth-order deformation Eq. 16  $m$  times with respect to  $q$ , then the resulting equation is divided  $m!$  and setting  $q = 0$ , we attain the  $m$ th-order deformation equation

$$L[x_m(\tau) - \chi_m x_{m-1}(\tau)] = \hbar R_m(\mathbf{u}_{m-1}, \boldsymbol{\omega}_{m-1}) \tag{24}$$

with the initial conditions

$$x_m(0) = 0, \quad x'_m(0) = 0 \quad (m \geq 1) \tag{25}$$

in which

$$\chi_m = \begin{cases} 0, & m \leq 1 \\ 1, & m > 1 \end{cases} \tag{26}$$

$$R_m(\mathbf{u}_{m-1}, \boldsymbol{\omega}_{m-1}) = \frac{1}{(m-1)!} \left. \frac{\partial^{m-1} N[x(\tau; q)]}{\partial q^{m-1}} \right|_{q=0} \tag{27}$$

It is found that  $R_m$  can also be written as

$$R_m(\mathbf{u}_{m-1}, \boldsymbol{\omega}_{m-1}) = \sum_{k=1}^{\varphi(m)} d_k(\omega_{m-1}) \cos(2k-1)\tau \tag{28}$$

where  $\varphi(m)$  is an integer that depends on  $m$ .

In view of the rule of solution expression and the linear operator  $L$ , the right hand side of Eq. 24 must not contain the terms of  $\cos\tau$ , otherwise the so-called secular terms such as  $\tau\cos\tau$  are available in the solutions. To avoid the presence of such terms, their coefficients are set to zero as follows

$$\frac{1}{\pi} \int_0^{2\pi} [\hbar R_m(\mathbf{u}_{m-1}, \boldsymbol{\omega}_{m-1})] \cos\tau \, d\tau = 0 \tag{29}$$

The solutions of  $\boldsymbol{\omega}_{m-1}$  ( $m = 1, 2, \dots$ ) in Eqs. 24 and 29 can be obtained successively. For the given values of  $\varepsilon_1, \varepsilon_2, \varepsilon_3, \varepsilon_4$  and  $A$ , the periodic solutions can be determined by the abovementioned analytical approach. We have

$$x_m(\tau) = \chi_m x_{m-1}(\tau) + \frac{\hbar}{\omega_0^2} \sum_{k=2}^{\varphi(m)} \frac{d_k(\omega_{m-1}) \cos(2k-1)\tau}{(1-(2k-1)^2)} + C_1 \cos\tau + C_0 \tag{30}$$

in which  $C_0$  and  $C_1$  can be determined by using the initial condition given in Eq. 25.



**Table 1** Comparison of the exact and approximate frequencies corresponding to various parameters in Eq. 8 for  $\hbar = -1$

Mode	$A$	$\varepsilon_1$	$\varepsilon_2$	$\varepsilon_3$	$\varepsilon_4$	$\omega_{\text{HPM}} = \omega_{\text{AFF}}$	$\omega_{\text{HAM}}$	$\omega_{\text{ex}}$
1	1.0	0.326845	0.129579	0.232598	0.087584	1.00705	1.01232	1.01015
2	0.5	1.642033	0.913055	0.313561	0.204297	0.93255	0.938636	0.93639
3	0.2	4.051486	1.665232	0.281418	0.149677	0.96546	0.966516	0.96664
4	0.3	8.205578	3.145368	0.272313	0.133708	0.85970	0.871382	0.86426

Hence, the  $m$ th-order approximations are

$$x(\tau) = \sum_{i=0}^m x_i(\tau), \quad \omega = \sum_{i=0}^m \omega_i \tag{31}$$

For  $m = 1$ , Eq. 29 becomes the following algebraic equations

$$\frac{A}{8} [8 - 8\omega_0^2 + A^2 (6\varepsilon_3 - 4\varepsilon_1\omega_0^2) + A^4 (5\varepsilon_4 - 3\varepsilon_2\omega_0^2)] = 0 \tag{32}$$

Solving Eq. 32 gives rise to

$$\omega_0 = \sqrt{\frac{6\varepsilon_3 A^2 + 5\varepsilon_4 A^4 + 8}{8 + 4\varepsilon_1 A^2 + 3\varepsilon_2 A^4}} \tag{33}$$

Making use of Eqs. 28 and 30 leads to

$$x_1(\tau) = \left( \frac{b_{1,3}\hbar}{8\omega_0^2} + \frac{b_{1,5}\hbar}{24\omega_0^2} \right) \cos \tau - \frac{b_{1,3}\hbar}{8\omega_0^2} \cos 3\tau - \frac{b_{1,5}\hbar}{24\omega_0^2} \cos 5\tau \tag{34}$$

where

$$b_{1,3} = \frac{A^3(16\varepsilon_3 - 15A^4\varepsilon_2\varepsilon_3 + 4A^2(5\varepsilon_4 - 7\varepsilon_2) - 10A^6\varepsilon_2\varepsilon_4 - 2\varepsilon_1(8\varepsilon_3A^2 + 5\varepsilon_4A^4 + 16))}{8(8 + 4\varepsilon_1A^2 + 3\varepsilon_2A^4)} \tag{35}$$

$$b_{1,5} = \frac{A^5((4 + 2A^2\varepsilon_1)\varepsilon_4 - 3\varepsilon_2(3\varepsilon_3A^2 + 2\varepsilon_4A^4 + 4))}{8(8 + 4\varepsilon_1A^2 + 3\varepsilon_2A^4)} \tag{36}$$

**Table 2** Comparison of the accuracy of approximate frequencies with exact solutions for  $\hbar = -1$

Mode	$A$	$\varepsilon_1$	$\varepsilon_2$	$\varepsilon_3$	$\varepsilon_4$	$\frac{ \omega_{\text{HPM}} - \omega_{\text{ex}} }{\omega_{\text{ex}}}$	$\frac{ \omega_{\text{HAM}} - \omega_{\text{ex}} }{\omega_{\text{ex}}}$
1	1.0	0.326845	0.129579	0.232598	0.087584	0.30664	0.21482
2	0.5	1.642033	0.913055	0.313561	0.204297	0.40947	0.23986
3	0.2	4.051486	1.665232	0.281418	0.149677	0.12144	0.01283
4	0.3	8.205578	3.145368	0.272313	0.133708	0.52752	0.82406

For  $m = 2$ , we substitute the solutions of  $x_0(\tau)$ ,  $x_1(\tau)$  and  $\omega_0$  into Eq. 29 to yield

$$\begin{aligned} \omega_1 = & \frac{\hbar}{10616832A(8 + 4A^2\varepsilon_1 + 3A^4\varepsilon_2)} \omega_0^9 \\ & \times \left( -(10287b_{1,3}^5 + 7965b_{1,3}^4b_{1,5} + 10962b_{1,3}^3b_{1,5}^2 + 5286b_{1,3}^2b_{1,5}^3 \right. \\ & + 1661b_{1,3}b_{1,5}^4 + 207b_{1,5}^5) \hbar^4\varepsilon_2 + 32A\hbar^2 \left( -(567b_{1,3}^4 + 729b_{1,3}^3b_{1,5} \right. \\ & + 738b_{1,3}^2b_{1,5}^2 + 303b_{1,3}b_{1,5}^3 + 52b_{1,5}^4) \hbar\varepsilon_2 + 30A(3b_{1,3} + b_{1,5}) \\ & \times (18b_{1,3}^2 + 12b_{1,3}b_{1,5} + 5b_{1,5}^2) \varepsilon_4 \omega_0^2 \\ & + 576\hbar(-8(72b_{1,3}^3 + 42b_{1,3}^2b_{1,5} + 44b_{1,3}b_{1,5}^2 + 9b_{1,5}^3) \hbar\varepsilon_1 \\ & + A^2(162b_{1,3}^3 + 18b_{1,3}^2b_{1,5} + 9b_{1,3}b_{1,5}^2 - b_{1,5}^3) \hbar\varepsilon_2 + 16A^3 \\ & \times (27b_{1,3}^2 + 24b_{1,3}b_{1,5} + 7b_{1,5}^2) \varepsilon_4 \omega_0^4 + 9216(9Ab_{1,3}^2\hbar(4\varepsilon_1 + 31A^2\varepsilon_2) \\ & + 12b_{1,3}(48 - 2Ab_{1,5}\hbar\varepsilon_1 + 14A_3b_{1,5}\hbar\varepsilon_2 + 72A^2\varepsilon_3 + 45A^4\varepsilon_4) \\ & + b_{1,5}(192 - 4Ab_{1,5}\hbar\varepsilon_1 + 75A^3b_{1,5}\hbar\varepsilon_2 + 432A^2\varepsilon_3 + 324A^4\varepsilon_4)) \omega_0^6 \\ & + 110592(-8(6b_{1,3} + 2b_{1,5} + A^2(-6b_{1,3} + b_{1,5})\varepsilon_1) \\ & \left. + 9A^4(7b_{1,3} + b_{1,5})\varepsilon_2) \omega_0^8 \right) \end{aligned} \tag{37}$$

From Eqs. 28 and 30, the first five terms result of  $R_2(\mathbf{u}_1, \omega_1)$  are derived in the following

$$R_2(\mathbf{u}_1, \omega_1) = b_{2,3} \cos 3\tau + b_{2,5} \cos 5\tau + b_{2,7} \cos 7\tau + b_{2,9} \cos 9\tau + b_{2,11} \cos 11\tau \tag{38}$$

where all coefficients  $b_{2,i}$  ( $i = 3, 5, 7, 9, 11$ ) are presented in Appendix. In addition, the solution of  $x_2(\tau)$  is

$$x_2(\tau) = x_1(\tau) + \frac{\hbar}{\omega_0^2} \sum_{k=1}^5 \frac{b_{2,2k+1} \cos(2k+1)\tau}{(1 - (2k+1)^2)} + C_1 \cos \tau + C_0 \tag{39}$$

in which  $C_0$  and  $C_1$  can be determined by the initial conditions in Eq. 25.

The higher-order approximations for  $\omega$  and  $x(\tau)$  ( $\omega_n$  and  $x_n(\tau)$ ,  $n \geq 2$ ) can be derived in a similar manner.

**Table 3** Comparison of the approximate frequencies using the optimal convergence-control parameter  $\hbar$  with exact solutions

Mode	$A$	$\varepsilon_1$	$\varepsilon_2$	$\varepsilon_3$	$\varepsilon_4$	$\hbar$	$\omega_{HAM}$	$\omega_{ex}$
1	1.0	0.326845	0.129579	0.232598	0.087584	-0.2820	1.01015	1.01015
2	0.5	1.642033	0.913055	0.313561	0.204297	-0.3084	0.93639	0.93639
3	0.2	4.051486	1.665232	0.281418	0.149677	-0.928	0.96652	0.96664
4	0.3	8.205578	3.145368	0.272313	0.133708	-0.1476	0.86426	0.86426

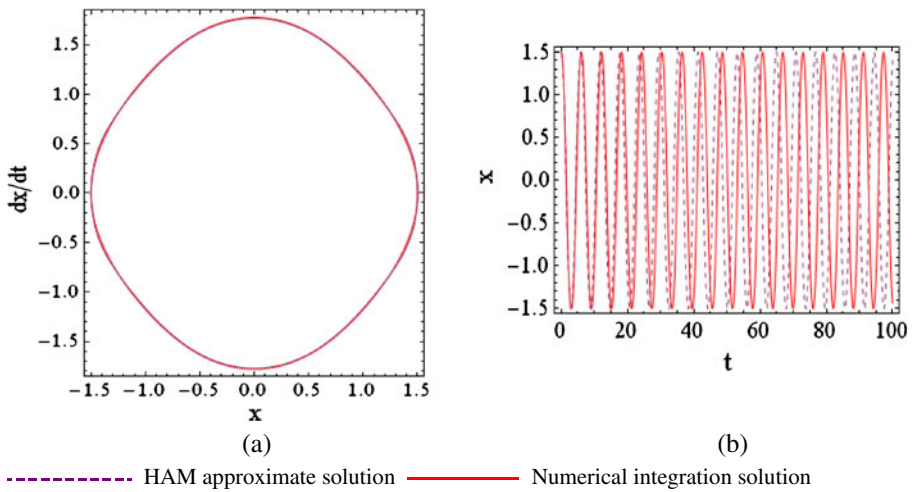


**Fig. 2** Comparison of the approximate and numerical integration solutions of Mode 1 for  $h = -1$  and  $A = 1.5$ . **a** Phase portrait diagram; **b** Time history response

Hitherto, there are a number of optimal HAM approaches, which can be able to achieve faster convergent homotopy-series solutions [19, 29]. For the periodic solutions of the nonlinear dynamical system in Eq. 8, the frequency  $\omega$  and the amplitude of vibration are the most important parameters to be concerned. In theory, the exact residual error of the  $m$ th-order of approximation can be defined as

$$\Delta_m = \left| \sum_{i=0}^m \omega_i - \omega_{ex} \right| \tag{40}$$

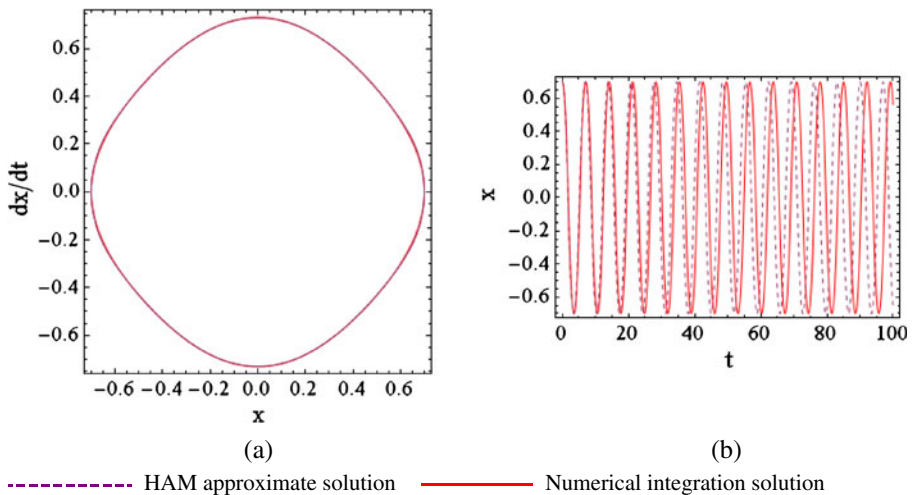


**Fig. 3** Comparison of the approximate and numerical integration solutions of Mode 2 for  $h = -1$  and  $A = 0.7$ . **a** Phase portrait diagram; **b** Time history response

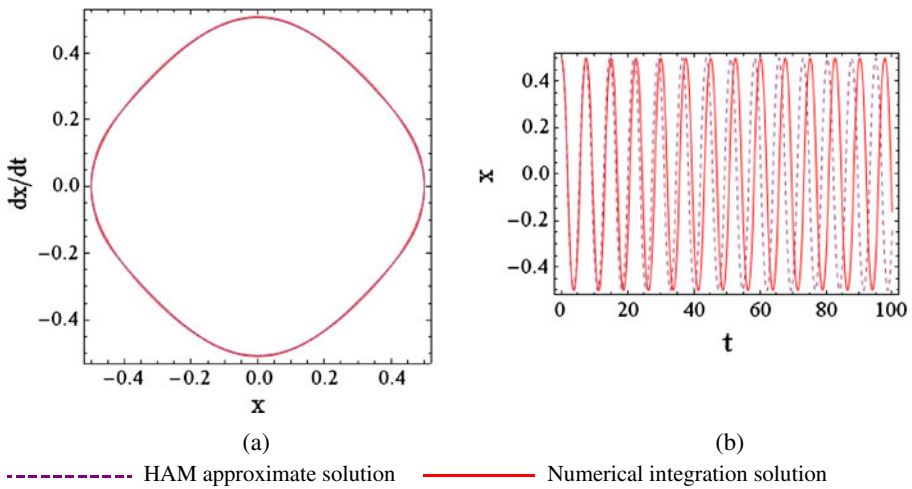


**Fig. 4** Comparison of the approximate and numerical integration solutions of Mode 3 for  $\hbar = -1$  and  $A = 0.5$ . **a** Phase portrait diagram; **b** Time history response

where  $\omega_{ex}$  is the exact nonlinear frequency of Eq. 8 derived using the numerical integration technique.

Because  $\Delta_m$  embraces the unknown convergence-control parameter  $\hbar$ ,  $\Delta_m$  decreases more rapidly to zero. Thus, the speed of the convergence for the corresponding homotopy-series solution is faster [19]. The corresponding value of the convergence-control parameter  $\hbar$  at the given order of approximation  $m$  can be optimized and selected by minimizing the residual error  $\Delta_m$ .

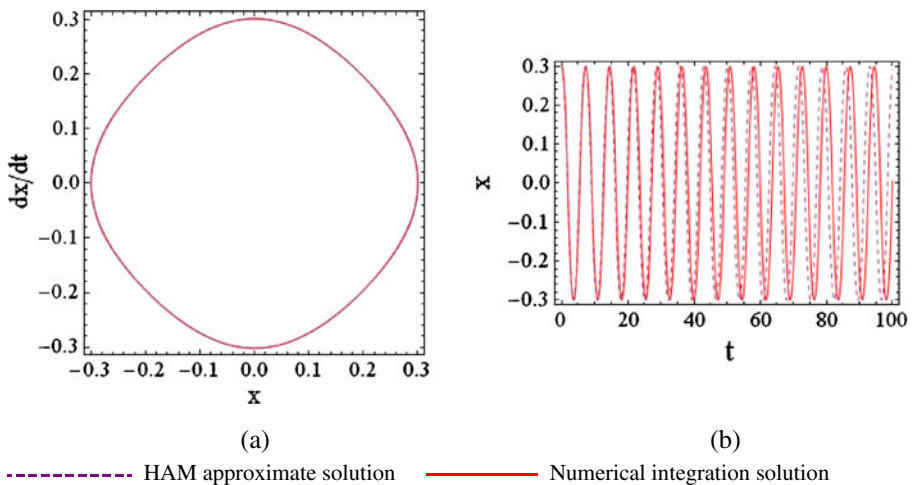


**Fig. 5** Comparison of the approximate and numerical integration solutions of Mode 4 for  $\hbar = -1$  and  $A = 0.3$ . **a** Phase portrait diagram; **b** Time history response

### 4 Results and discussion

In this section, we compare the asymptotic analytical solutions obtained by the HAM vis-à-vis the numerical integration and published analytical solutions. The results of amplitude–frequency formulation  $\omega_{AFF}$  [6], homotopy perturbation method  $\omega_{HPM}$  [6], present approach  $\omega_{HAM}$  and exact solution  $\omega_{ex}$  [6] are tabulated in Table 1 for various parameters  $\varepsilon_i$  ( $i = 1-4$ ) and amplitudes of vibration  $A$ . The values of dimensionless parameters  $\varepsilon_i$  ( $i = 1-4$ ) in Table 1 correspond to the first four vibration modes (Modes 1–4) of the restrained cantilever beam. More set of data for  $\varepsilon_i$  ( $i = 1-4$ ) resulting from different dimensionless stiffness parameter  $S = Kl/(EI)$  [8], mass ratio  $\mu$  and relative position  $\eta$  of the intermediate mass  $M$  can be found in Table 2 of Ref. [8]. To verify the accuracy and correctness of the HAM in this paper, we confine the focus on the cases as stated in Table 1.

In comparing with the exact solutions  $\omega_{ex}$ , Table 1 shows that the second order HAM solutions  $\omega_{HAM}$  for  $\hbar = -1$  are better than the first-order solutions of  $\omega_{AFF}$  and  $\omega_{HPM}$  in the first three cases. The relative errors of  $\omega_{HAM}$  and  $\omega_{HPM}$  with respect to  $\omega_{ex}$  are demonstrated in Table 2. Nonetheless, the lower-order solutions of  $\omega_{AFF}$  and  $\omega_{HPM}$  are slightly better than  $\omega_{HAM}$  in the fourth case. The reason is mainly due to the fact that the second-order solution  $\omega_{HAM}$  cannot converge very well for  $\hbar = -1$  in this case. By making use of Eq. 40 to optimize the convergence-control parameter  $\hbar$  to  $-0.1476$ , we observe that the

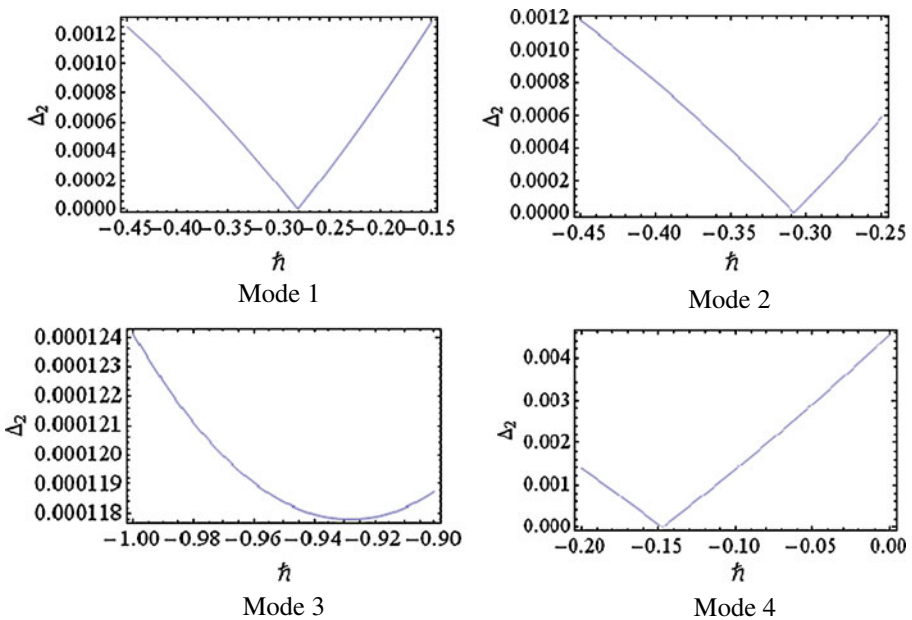


**Fig. 6** The selection of optimal convergence-control parameters  $\hbar$  in Table 3 for Modes 1–4

solution of  $\omega_{HAM}$  is exactly the same as  $\omega_{ex}$  shown in Table 3. The results of  $\omega_{HAM}$  for the first three cases are also refined in using the optimal parameters  $\hbar$ . In principle, the basic philosophy of the homotopy perturbation method (HPM) is exactly the same as the homotopy analysis method for  $\hbar = -1$ . Thus, the HPM is regarded as a special kind of the HAM [18]. It is believed that the construction of higher-order HPM solutions [6] can improve the accuracy in solving Eq. 8 as well, yet these solutions cannot readily converge to desired accuracy for large amplitudes of motion. For the HAM, the auxiliary parameter  $\hbar$  can be adjusted and controlled to speed up the convergence of solutions. The value of  $\hbar$  is one of the dominant factors in the HAM to extend its validity and flexibility. This also explains why the rigorous investigation of the fifth-order nonlinear equation shall be revisited in this paper using the HAM. Although not presented here, it has been checked that a coupling of the second-order HAM solutions with the Padé approximant [17, 24] is rather

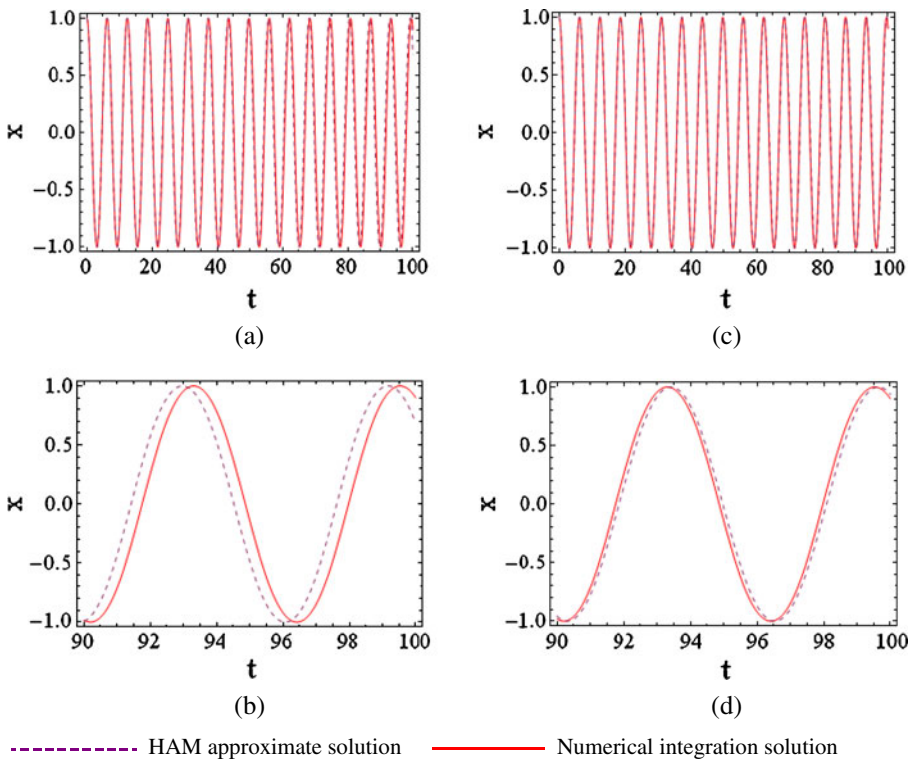


**Fig. 7** Comparison of time history responses of the approximate and numerical integration solutions of Mode 1 for  $A = 1$ . **a** and **b**  $\hbar = -1$ ; **c** and **d**  $\hbar = -0.2820$

difficult to accelerate the convergence of the solutions for the cases given in Table 1, for instance using the [2, 2] homotopy Padé approximant.

In Figs. 2, 3, 4 and 5, the phase portrait diagrams and time history responses for a number of cases governed by different amplitudes of vibration and  $\bar{h} = -1$  are depicted. We can clearly observe that the second-order HAM solutions are in good agreement with the numerical integration solutions. It is emphasized that the variables  $t$  and  $x$  in all figures of this paper are, respectively, the dimensionless time  $\bar{t}$  and dimensionless deflection at the beam tip  $\bar{x}$  as stated in Eqs. 8 and 9. To further manifest the vital role of the convergence-control parameter  $\bar{h}$  in the HAM, several examples selected from Table 3 are presented for illustration in Figs. 6, 7, 8, 9 and 10. Figure 6 displays the selection of optimal value of  $\bar{h}$  for the examples given in Table 3. In Figs. 7, 8, 9 and 10, we demonstrate the accuracy of periodic solutions of the HAM using  $\bar{h} = -1$  and the optimal parameter  $\bar{h}$ . For the initial time domain, both the solutions for  $\bar{h} = -1$  and its optimal value agree well with the numerical integration solutions. However, the deviations between the solutions of the HAM for

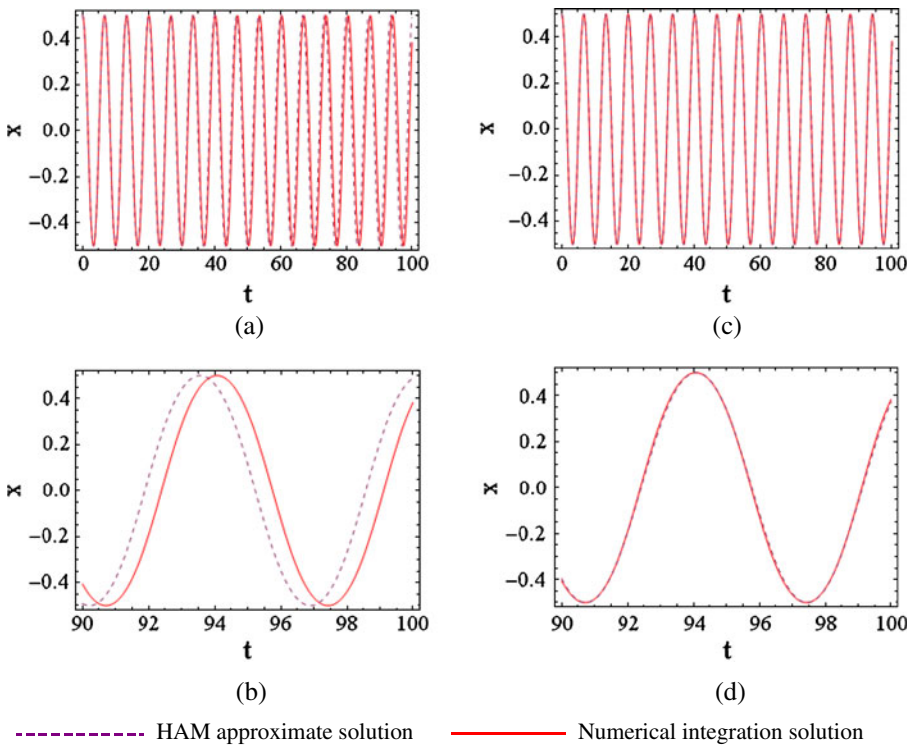


**Fig. 8** Comparison of time history responses of the approximate and numerical integration solutions of Mode 2 for  $A = 0.5$ . **a** and **b**  $\bar{h} = -1$ ; **c** and **d**  $\bar{h} = -0.3084$

$\hbar = -1$  and numerical integration technique obviously increase when time progresses to large domain  $t \in [90, 100]$  in Figs. 7b, 8b and 10b. Because the parameter  $\hbar = -1$  is almost equal to the optimal value  $\hbar = -0.928$ , thus the periodic solution for  $\hbar = -1$  in Fig. 9b is very accurate during large time domain. In Figs. 7d, 8d, 9d and 10d, the solutions of optimal parameter  $\hbar$  still have good performance with respect to the numerical ones even in large time domain.

The higher-order HAM solutions are required and constructed when subjected to large amplitudes of motion, such that the accuracy of the approximations can be maintained. In Figs. 11 and 12, the third-order HAM solutions of Mode 1 (i.e.  $\varepsilon_1 = 0.326845$ ,  $\varepsilon_2 = 0.129579$ ,  $\varepsilon_3 = 0.232598$ ,  $\varepsilon_4 = 0.087584$ ) are presented for  $A = 3$  and 5. Despite the optimization of the parameter  $\hbar$  is capable of using Eq. 40, this parameter can also be determined by plotting the  $\omega-h$  curve. In Fig. 11a, the valid region is  $\hbar \in [-0.7, 0.5]$  for  $A = 3$ , thus  $\hbar = -0.075$  is selected for computation in this case. It is evident that the

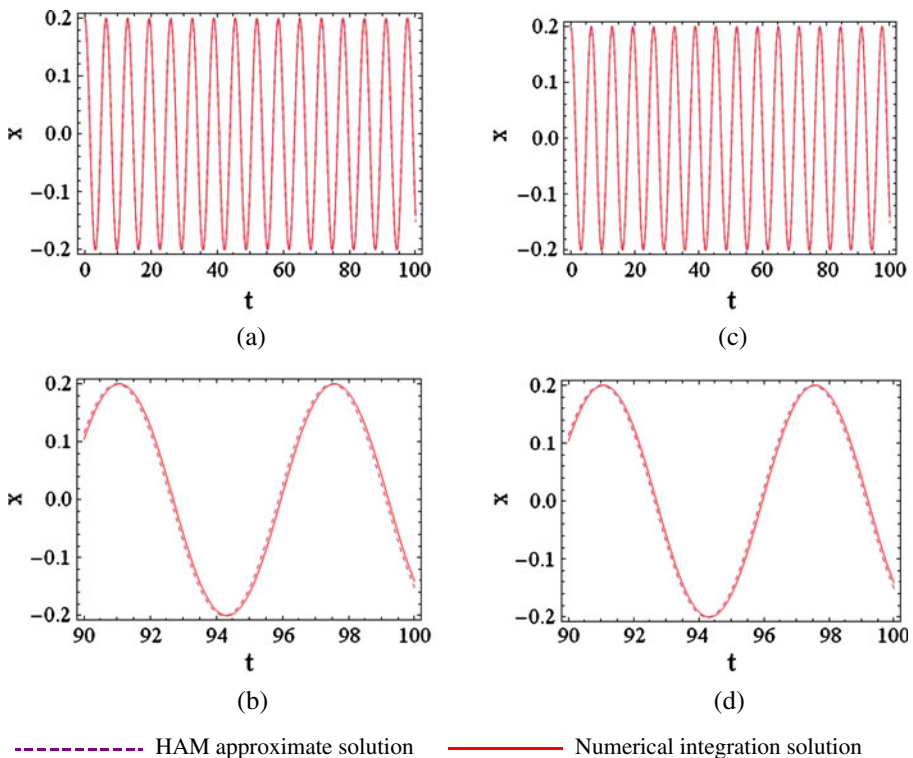


**Fig. 9** Comparison of time history responses of the approximate and numerical integration solutions of Mode 3 for  $A = 0.2$ . **a** and **b**  $\hbar = -1$ ; **c** and **d**  $\hbar = -0.928$



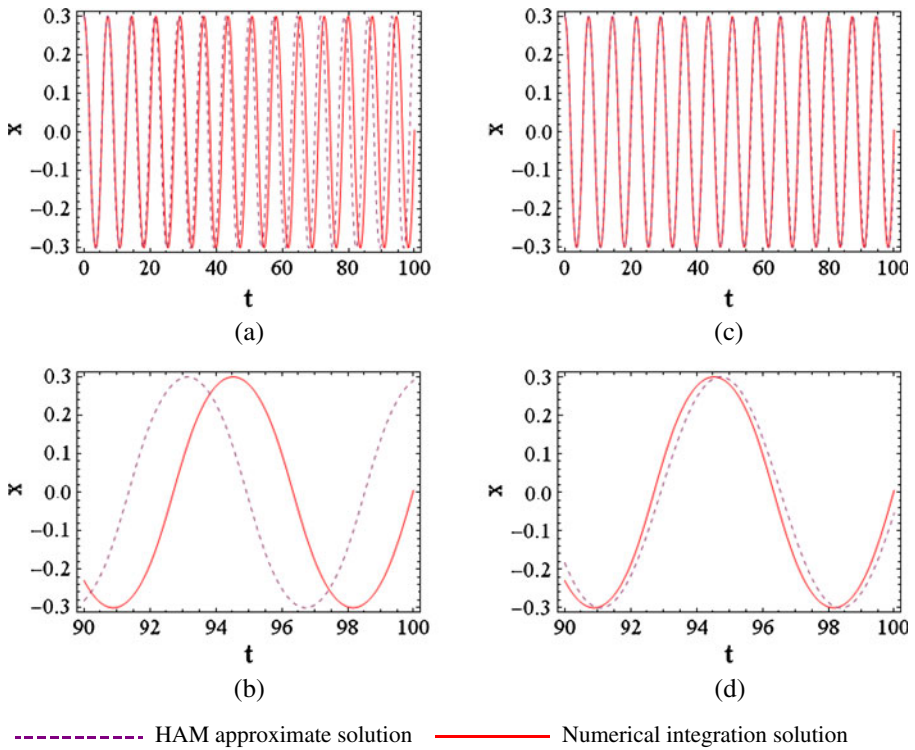


**Fig. 10** Comparison of time history responses of the approximate and numerical integration solutions of Mode 4 for  $A = 0.3$ . **a** and **b**  $\hat{h} = -1$ ; **c** and **d**  $\hat{h} = -0.1476$

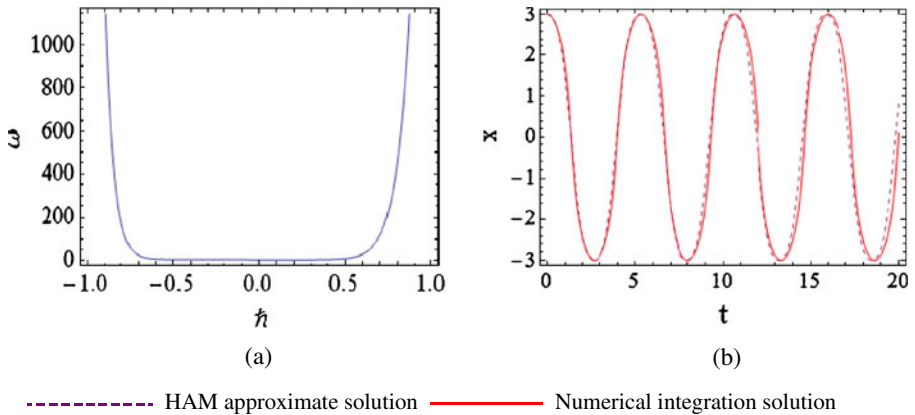


**Fig. 11** **a** The third-order HAM approximation of  $\omega$ - $\hat{h}$  curve for  $A = 3$ ; **b** comparison of time history responses of Mode 1 for  $A = 3$  and  $\hat{h} = -0.075$

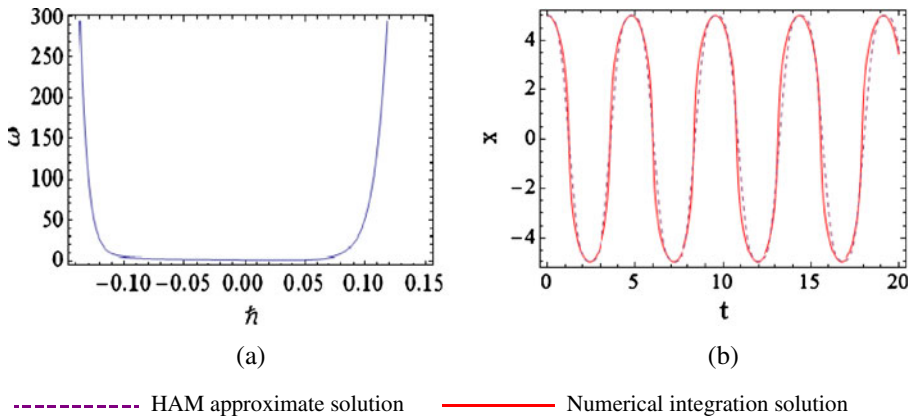


**Fig. 12** **a** The third-order HAM approximation of  $\omega$ - $\hbar$  curve for  $A = 5$ ; **b** Comparison of time history responses of Mode 1 for  $A = 5$  and  $\hbar = -0.015$

third-order approximate result is in good agreement as compared to the numerical integration solution in Fig. 11b. Similar observation can be viewed in Fig. 12 for  $A = 5$  and  $\hbar = -0.015$ .

## 5 Conclusions

The fifth-order Duffing type temporal problem containing strongly inertial and static nonlinearities has been intensively studied by the HAM. The nonlinear frequencies and periodic motions of various vibration modes for elastically restrained beams carrying the lumped mass are presented. The HAM is dissimilar to the classical perturbation approaches, its range of validity is capable of handling problems with strong nonlinearities. The purposes of this paper not only formulate the asymptotic approximate solutions for the strongly nonlinear system, but also furnish a guidance to establish the higher-order asymptotic analytical approximations if necessary. Moreover, it is found that the accuracy of the HAM is greatly affected by the selection of appropriate convergence-control parameter  $\hbar$ . To further improve the accuracy of solutions, the parameter  $\hbar$  can be optimized and determined by the minimization of the residual error  $\Delta_m$  for any given order approximation  $m$ . Ultimately, illustrative examples are used as crucial evidence to support that the HAM is effective for the quantitative analysis of strongly nonlinear problems.

**Acknowledgements** The authors, YHQ and WZ, gratefully acknowledge the support of the National Natural Science Foundation for Distinguished Young Scholars of China (NNSFDYSC) through grant No.10425209, the National Natural Science Foundations of China (NNSFC) through grants No.10732020 and No.11072008, the Funding Project for Academic Human Resources Development Institutions of Higher Learning under the Jurisdiction of Beijing Municipality (PHRIHLB), and the Foundation of Zhejiang Educational Committee through grant No.Y200909156. The authors, SKL and YX, gratefully appreciate the financial support from the University of Western Sydney through a Research Grant Scheme (Project No. 20731-80749).

### Appendix

The coefficients  $b_{2,i}$  ( $i = 3, 5, 7, 9, 11$ ) in Eq. 38 are presented as follows:

$$\begin{aligned}
 b_{2,3} = \frac{1}{127401984\omega_0^8} & (60993b_{1,3}^5\hbar^5\varepsilon_2 + 203b_{1,5}^5\hbar^5\varepsilon_2 + 2712Ab_{1,5}^4\hbar^4\varepsilon_2\omega_0^2 \\
 & + 81b_{1,3}^4\hbar^4\varepsilon_2(205b_{1,5}\hbar + 2376A\omega_0^2) + 13824Ab_{1,5}^2\hbar^2\omega_0^4 \\
 & \times (56\varepsilon_1\omega_0^2 - A^2(\varepsilon_4 - 107\varepsilon_2\omega_0^2)) + 2304b_{1,5}^3\hbar^3\omega_0^2(16\varepsilon_1\omega_0^2 \\
 & - A^2(\varepsilon_4 - 21\varepsilon_2\omega_0^2)) + 331776A^2b_{1,5}\hbar\omega_0^6(72\varepsilon_1\omega_0^2 + A^2 \\
 & \times (3\varepsilon_4 + 73\varepsilon_2\omega_0^2)) + 3b_{1,3}\hbar(833b_{1,5}^4\hbar^4\varepsilon_2 + 7488Ab_{1,5}^3\hbar^3\varepsilon_2\omega_0^2 \\
 & + 55296Ab_{1,5}\hbar\omega_0^4(28\varepsilon_1\omega_0^2 - A^2(\varepsilon_4 - 47\varepsilon_2\omega_0^2)) + 331776\omega_0^6 \\
 & \times (16(-1 + 9\omega_0^2) + A^2(-12\varepsilon_3 + 64\varepsilon_1\omega_0^2) + A^4(-3\varepsilon_4 + 47\varepsilon_2\omega_0^2)) \\
 & + 576b_{1,5}^2\hbar^2\omega_0^2(296\varepsilon_1\omega_0^2 + A^2(-15\varepsilon_4 + 173\varepsilon_2\omega_0^2))) + 54b_{1,3}^3\hbar^3 \\
 & \times (617b_{1,5}^2\hbar^2\varepsilon_2 + 2208Ab_{1,5}\hbar\varepsilon_2\omega_0^2 + 576(72\varepsilon_1\omega_0^4 + A^2 \\
 & \times (-5\varepsilon_4\omega_0^2 + 23\varepsilon_2\omega_0^4))) + 18b_{1,3}^2\hbar^2(493b_{1,5}^3\hbar^3\varepsilon_2 \\
 & + 4968Ab_{1,5}^2\hbar^2\varepsilon_2\omega_0^2 + 288b_{1,5}\hbar\omega_0^2(32\varepsilon_1\omega_0^2 + A^2(-15\varepsilon_4 \\
 & + 157\varepsilon_2\omega_0^2)) + 27648(18A\varepsilon_1\omega_0^6 + A^3(-\varepsilon_4\omega_0^4 + 11\varepsilon_2\omega_0^6))) \\
 & - 15925248A^3 \times (8\varepsilon_1 + 7A^2\varepsilon_2)\omega_0^9\omega_1), \tag{41}
 \end{aligned}$$

$$\begin{aligned}
 b_{2,5} = \frac{1}{42467328\omega_0^8} & (-2187b_{1,3}^5\hbar^5\varepsilon_2 + 307b_{1,5}^5\hbar^5\varepsilon_2 + 3304Ab_{1,5}^4\hbar^4\varepsilon_2\omega_0^2 + 27b_{1,3}^4\hbar^4\varepsilon_2 \\
 & \times (931b_{1,5}\hbar - 600A\omega_0^2) + 110592b_{1,5}\hbar\omega_0^6(-16 + 400\omega_0^2 - 8A^2 \\
 & \times (3\varepsilon_3 - 25\varepsilon_1\omega_0^2) - 3A^4(5\varepsilon_4 - 49\varepsilon_2\omega_0^2)) + 4608Ab_{1,5}^2\hbar^2\omega_0^4 \\
 & \times (208\varepsilon_1\omega_0^2 + A^2(-11\varepsilon_4 + 153\varepsilon_2\omega_0^2)) + 192b_{1,5}^3\hbar^3\omega_0^2 \\
 & \times (408\varepsilon_1\omega_0^2 + A^2(-23\varepsilon_4 + 205\varepsilon_2\omega_0^2)) + 54b_{1,3}^3\hbar^3(255b_{1,5}^2\hbar^2\varepsilon_2 \\
 & + 1472Ab_{1,5}\hbar\varepsilon_2\omega_0^2 - 96(16\varepsilon_1\omega_0^4 + 5A^2\omega_0^2(\varepsilon_4 + 5\varepsilon_2\omega_0^2))) \\
 & + 6b_{1,3}^2\hbar^2(1613b_{1,5}^3\hbar^3\varepsilon_2 + 8616Ab_{1,5}^2\hbar^2\varepsilon_2\omega_0^2 - 27648(2A\varepsilon_1\omega_0^6 \\
 & + A^3\omega_0^4(\varepsilon_4 + 5\varepsilon_2\omega_0^2)) + 576b_{1,5}\hbar\omega_0^2(268\varepsilon_1\omega_0^2 + A^2(-15\varepsilon_4 \\
 & + 85\varepsilon_2\omega_0^2))) + b_{1,3}\hbar(2459b_{1,5}^4\hbar^4\varepsilon_2 + 22464Ab_{1,5}^3\hbar^3\varepsilon_2\omega_0^2 \\
 & + 995328A^2\omega_0^6(-4\varepsilon_3 + 16\varepsilon_1\omega_0^2 - 3A^2(\varepsilon_4 - 5\varepsilon_2\omega_0^2)) \\
 & + 27648Ab_{1,5}\hbar\omega_0^4(136\varepsilon_1\omega_0^2 + A^2(-7\varepsilon_4 + 73\varepsilon_2\omega_0^2)) \\
 & + 1152b_{1,5}^2\hbar^2\omega_0^2(244\varepsilon_1\omega_0^2 + A^2(-21\varepsilon_4 + 163\varepsilon_2\omega_0^2))) \\
 & - 15925248A^5\varepsilon_2\omega_0^9\omega_1), \tag{42}
 \end{aligned}$$

$$\begin{aligned}
b_{2,7} = & -\frac{1}{42467328\omega_0^8} \hbar (22113b_{1,3}^5 \hbar^4 \varepsilon_2 + 27b_{1,3}^4 \hbar^3 \varepsilon_2 (875b_{1,5} \hbar + 2928A\omega_0^2) + b_{1,3} \\
& \times (-761b_{1,5}^4 \hbar^4 \varepsilon_2 - 2976Ab_{1,5}^3 \hbar^3 \varepsilon_2 \omega_0^2 - 995328A^4 \omega_0^6 \\
& \times (-\varepsilon_4 + 5\varepsilon_2 \omega_0^2) + 2304b_{1,5}^2 \hbar^2 \omega_0^2 (-46\varepsilon_1 \omega_0^2 + A^2 \\
& \times (3\varepsilon_4 + 5\varepsilon_2 \omega_0^2)) + 55296Ab_{1,5} \hbar \omega_0^4 (28\varepsilon_1 \omega_0^2 + A^2 \\
& \times (\varepsilon_4 + 29\varepsilon_2 \omega_0^2))) - 48b_{1,5} (3b_{1,5}^4 \hbar^4 \varepsilon_2 + 35Ab_{1,5}^3 \hbar^3 \varepsilon_2 \omega_0^2 \\
& + 27648A^2 \omega_0^6 (-\varepsilon_3 + 10\varepsilon_1 \omega_0^2 - A^2 (\varepsilon_4 - 10\varepsilon_2 \omega_0^2)) \\
& + 16b_{1,5}^2 \hbar^2 \omega_0^2 (38\varepsilon_1 \omega_0^2 + A^2 (-3\varepsilon_4 + 23\varepsilon_2 \omega_0^2)) \\
& + 96Ab_{1,5} \hbar \omega_0^4 (144\varepsilon_1 \omega_0^2 + A^2 (-7\varepsilon_4 + 69\varepsilon_2 \omega_0^2))) \\
& + 54b_{1,3}^2 \hbar^2 (91b_{1,5}^2 \hbar^2 \varepsilon_2 + 1712Ab_{1,5} \hbar \varepsilon_2 \omega_0^2 + 96 \\
& \times (136\varepsilon_1 \omega_0^4 + A^2 (-5\varepsilon_4 \omega_0^2 + 71\varepsilon_2 \omega_0^4))) + 6b_{1,3}^2 \hbar \\
& \times (127b_{1,5}^3 \hbar^3 \varepsilon_2 + 2112Ab_{1,5}^2 \hbar^2 \varepsilon_2 \omega_0^2 + 288b_{1,5} \hbar \omega_0^2 \\
& \times (320\varepsilon_1 \omega_0^2 + A^2 (-3\varepsilon_4 + 233\varepsilon_2 \omega_0^2)) + 6912 \\
& \times (72A\varepsilon_1 \omega_0^6 + A^3 (-\varepsilon_4 \omega_0^4 + 59\varepsilon_2 \omega_0^6))), \quad (43)
\end{aligned}$$

$$\begin{aligned}
b_{2,9} = & \frac{1}{14155776\omega_0^8} \hbar (4887b_{1,3}^5 \hbar^4 \varepsilon_2 - 243b_{1,3}^4 \hbar^3 \varepsilon_2 (35b_{1,5} \hbar - 48A\omega_0^2) \\
& - b_{1,5} (79b_{1,5}^4 \hbar^4 \varepsilon_2 + 1040Ab_{1,5}^3 \hbar^3 \varepsilon_2 \omega_0^2 \\
& - 36864A^4 \omega_0^6 (-3\varepsilon_4 + 35\varepsilon_2 \omega_0^2) + 1536Ab_{1,5} \hbar \omega_0^4 \\
& \times (200\varepsilon_1 \omega_0^2 - A^2 \times (\varepsilon_4 - 179\varepsilon_2 \omega_0^2)) + 384b_{1,5}^2 \hbar^2 \omega_0^2 \\
& \times (44\varepsilon_1 \omega_0^2 - A^2 (\varepsilon_4 - 39\varepsilon_2 \omega_0^2))) - 18b_{1,3}^2 \hbar^2 \\
& \times (433b_{1,5}^2 \hbar^2 \varepsilon_2 + 1872Ab_{1,5} \hbar \varepsilon_2 \omega_0^2 - 96 (72\varepsilon_1 \omega_0^4 \\
& + A^2 \omega_0^2 (\varepsilon_4 + 5\varepsilon_2 \omega_0^2))) - 6b_{1,3}^2 \hbar (599b_{1,5}^3 \hbar^3 \varepsilon_2 \\
& + 4896Ab_{1,5}^2 \hbar^2 \varepsilon_2 \omega_0^2 + 2304A^3 \omega_0^4 \times (-\varepsilon_4 + 27\varepsilon_2 \omega_0^2) \\
& + 96b_{1,5} \hbar \omega_0^2 (464\varepsilon_1 \omega_0^2 + A^2 (-15\varepsilon_4 + 301\varepsilon_2 \omega_0^2))) \\
& - 12b_{1,3} b_{1,5} \hbar (73b_{1,5}^3 \hbar^3 \varepsilon_2 + 744Ab_{1,5}^2 \hbar^2 \varepsilon_2 \omega_0^2 \\
& + 32b_{1,5} \hbar \omega_0^2 (364\varepsilon_1 \omega_0^2 - 9A^2 (\varepsilon_4 - 31\varepsilon_2 \omega_0^2)) \\
& + 1536 (64A\varepsilon_1 \omega_0^6 + A^3 (-\varepsilon_4 \omega_0^4 + 59\varepsilon_2 \omega_0^6))), \quad (44)
\end{aligned}$$

$$\begin{aligned}
 b_{2,11} = & \frac{1}{42467328\omega_0^8} \hbar^2 (5751b_{1,3}^5 \hbar^3 \varepsilon_2 + 27b_{1,3}^4 \hbar^2 \varepsilon_2 (1265b_{1,5} \hbar + 1176A\omega_0^2) \\
 & - 24b_{1,3}^2 b_{1,5} \hbar (167b_{1,5}^2 \hbar^2 \varepsilon_2 + 714Ab_{1,5} \hbar \varepsilon_2 \omega_0^2 \\
 & - 576(41\varepsilon_1 + 10A^2 \varepsilon_2) \omega_0^4) + 54b_{1,3}^3 \hbar (13b_{1,5}^2 \hbar^2 \varepsilon_2 \\
 & + 1664Ab_{1,5} \hbar \varepsilon_2 \omega_0^2 + 96A^2 \omega_0^2 (-\varepsilon_4 + 27\varepsilon_2 \omega_0^2)) \\
 & - 16b_{1,3} b_{1,5} (137b_{1,5}^3 \hbar^3 \varepsilon_2 + 1284Ab_{1,5}^2 \hbar^2 \varepsilon_2 \omega_0^2 \\
 & + 1728A^3 \omega_0^4 (-\varepsilon_4 + 47\varepsilon_2 \omega_0^2) + 144b_{1,5} \hbar \omega_0^2 (86\varepsilon_1 \omega_0^2 \\
 & + A^2 (-3\varepsilon_4 + 79\varepsilon_2 \omega_0^2))) - 2b_{1,5}^2 (161b_{1,5}^3 \hbar^3 \varepsilon_2 \\
 & + 2088Ab_{1,5}^2 \hbar^2 \varepsilon_2 \omega_0^2 + 2304(200A\varepsilon_1 \omega_0^6 - 3A^3 \omega_0^4 \\
 & \times (\varepsilon_4 - 75\varepsilon_2 \omega_0^2)) + 96b_{1,5} \hbar \omega_0^2 (344\varepsilon_1 \omega_0^2 + A^2 \\
 & \times (-9\varepsilon_4 + 323\varepsilon_2 \omega_0^2))))). \tag{45}
 \end{aligned}$$

**References**

1. Abdulaziz, O., Noor, N.F.M., Hashim, I.: Homotopy analysis method for fully developed MHD micropolar fluid flow between vertical porous plates. *Int. J. Numer. Methods Eng.* **78**, 817–827 (2009)
2. Amore, P., Aranda, A.: Improved Lindstedt–Poincaré method for the solution of nonlinear problems. *J. Sound Vib.* **283**, 1115–1136 (2005)
3. Chen, S.S., Chen, C.K.: Application of the differential transformation method to the free vibrations of strongly non-linear oscillators. *Nonlinear Anal.: Real World Appl.* **10**, 881–888 (2009)
4. Chen, Y.M., Liu, J.K.: Homotopy analysis method for limit cycle flutter of airfoils. *Appl. Math. Comput.* **203**, 854–863 (2008)
5. Cheung, Y.K., Chen, S.H., Lau, S.L.: A modified Lindstedt–Poincaré method for certain non-linear oscillators. *Int. J. Non-Linear Mech.* **26**, 367–378 (1991)
6. Ganji, S.S., Ganji, D.D., Sfehiani, M.G., Karimpour, S.: Application of AFF and HPM to the systems of strongly nonlinear oscillation. *Current Applied Physics* **10**, 1317–1325 (2010)
7. Hamdan, M.N., Dado, M.H.F.: Large amplitude free vibrations of a uniform cantilever beam carrying an intermediate lumped mass and rotary inertia. *J. Sound Vib.* **206**, 151–168 (1997)
8. Hamdan, M.N., Shabaneh, N.H.: On the large amplitude free vibrations of a restrained uniform beam carrying an intermediate lumped mass. *J. Sound Vib.* **199**, 711–736 (1997)
9. Hilton, P.J.: *An Introduction to Homotopy Theory*. Cambridge University Press, Cambridge (1953)
10. Hu, Q.Q., Lim, C.W., Chen, L.Q.: Nonlinear vibration of a cantilever with a Derjaguin–Müller–Toporov contact end. *Int. J. Struct. Stab. Dyn.* **8**, 25–40 (2008)
11. Huseyin, K., Lin, R.: An intrinsic multiple-scale harmonic balance method for non-linear vibration and bifurcation problems. *Int. J. Non-Linear Mech.* **26**, 727–740 (1991)
12. Jafari-Talookolaei, R.A., Salarieh, H., Kargarnovin, M.H.: Analysis of large amplitude free vibrations of unsymmetrically laminated composite beams on a nonlinear elastic foundation. *Acta Mech.* doi:10.1007/s00707-010-0439-x (to appear)
13. Ke, L.L., Yang, J., Kitipornchai, S., Xiang, Y.: Flexural vibration and elastic buckling of a cracked Timoshenko beam made of functionally graded materials. *Mech. Adv. Mater. Struct.* **16**, 488–502 (2009)

14. Lai, S.K., Lim, C.W., Wu, B.S., Wang, C., Zeng, Q.C., He, X.F.: Newton-harmonic balancing approach for accurate solutions to nonlinear cubic–quintic Duffing oscillators. *Appl. Math. Model.* **33**, 852–866 (2009)
15. Liao, S.J.: The proposed homotopy analysis techniques for the solution of nonlinear problems. Ph.D. dissertation, Shanghai Jiao Tong University, China (1992)
16. Liao, S.J.: An approximate solution technique not depending on small parameters: a special example. *Int. J. Non-Linear Mech.* **30**, 371–380 (1995)
17. Liao, S.J.: *Beyond Perturbation: Introduction to the Homotopy Analysis Method*. Chapman & Hall, Boca Raton (2003)
18. Liao, S.J.: Comparison between the homotopy analysis method and homotopy perturbation method. *Appl. Math. Comput.* **169**, 1186–1194 (2005)
19. Liao, S.J.: An optimal homotopy-analysis approach for strongly nonlinear differential equations. *Commun. Nonlinear Sci. Numer. Simul.* **15**, 2003–2016 (2010)
20. Lim, C.W., Xu, R., Lai, S.K., Yu, Y.M., Yang, Q.: Nonlinear free vibration of an elastically-restrained beam with a point via the Newton-harmonic balancing approach. *Int. J. Nonlinear Sci. Numer. Simul.* **10**, 661–674 (2009)
21. Mehdipour, I., Ganji, D.D., Mozaffari, M.: Application of the energy balance method to nonlinear vibrating equations. *Curr. Appl. Phys.* **10**, 104–112 (2010)
22. Mickens, R.E.: *Mathematical Methods for the Natural and Engineering Sciences*. World Scientific, Singapore (2004)
23. Nash, C., Sen, S.: *Topology and Geometry for Physicists*. Academic, London (1983)
24. Pirbodaghi, T., Hoseini, S.H., Ahmadian, M.T., Farrahi, G.H.: Duffing equations with cubic and quintic nonlinearities. *Comput. Math. Appl.* **57**, 500–506 (2009)
25. Pušenjak, R.R.: Extended Lindstedt–Poincaré method for non-stationary resonances of dynamical systems with cubic nonlinearities. *J. Sound Vib.* **314**, 194–216 (2008)
26. Seelig, F.F.: Unrestricted harmonic balance II. Application to stiff ordinary differential equations in enzyme catalysis. *J. Math. Biol.* **12**, 187–198 (1981)
27. Senator, M., Bapat, C.N.: A perturbation technique that works even when the non-linearity is not small. *J. Sound Vib.* **164**, 1–27 (1993)
28. Summers, J.L., Savage, M.D.: Two timescale harmonic-balance. I. Application to autonomous one-dimensional nonlinear oscillators. *Philos. Trans. R. Soc. A: Math. Phys. Eng. Sci.* **340**, 473–501 (1992)
29. Van Gorder, R.A., Vajravelu, K.: On the selection of auxiliary functions, operators, and convergence control parameters in the application of the homotopy analysis method to nonlinear differential equations: a general approach. *Commun. Nonlinear Sci. Numer. Simul.* **14**, 4078–4089 (2009)
30. Wagner, H.: Large-amplitude free vibrations of a beam. *J. Appl. Mech. Trans. ASME* **32**, 887–892 (1965)
31. Wang, C., Pop, I.: Analysis of the flow of a power-law fluid film on an unsteady stretching surface by means of homotopy analysis method. *J. Non-Newton. Fluid Mech.* **138**, 161–172 (2006)
32. Wu, B.S., Li, P.S.: A method for obtaining approximate analytic periods for a class of nonlinear oscillators. *Meccanica* **36**, 167–176 (2001)
33. Yabushita, K., Yamashita, M., Tsuboi, K.: An analytic solution of projectile motion with the quadratic resistance law using the homotopy analysis method. *J. Phys. A: Math. Theory* **40**, 8403–8416 (2007)
34. Zhang, W., Qian, Y.H., Yao, M.H., Lai, S.K.: Periodic solutions of multi-degree-of-freedom strongly nonlinear coupled van der Pol oscillators by homotopy analysis method. *Acta Mech.* **217**, 269–285 (2011)
35. Zhang, W., Wang, F.X., Yao, M.H.: Global bifurcations and chaotic dynamics in nonlinear nonplanar oscillations of a parametrically excited cantilever beam. *Nonlinear Dyn.* **40**, 251–279 (2005)